Unsteady Flame and Flow Field Interaction of a Premixed Model Gas Turbine Burner

K.-U. Schildmacher[1], A. Hoffmann[2], L. Selle[3],
R. Koch[4], C. Schulz[5], H.-J. Bauer[4], T. Poinsot[6]

[1]*Siemens Power Generation, Muelheim, Germany*
[2]*PCI, University of Heidelberg, Germany*
[3]*California Institute of Technology, Pasadena, California, USA*
[4]*Institute of Thermal Turbomachinery, University of Karlsruhe, Germany*
[5]*IVG, University of Duisburg-Essen, Germany*
[6]*CERFACS, Toulouse, France*

Abstract

In recent years, the NO_x emissions of heavy duty gas turbines have been significantly reduced by introducing lean premixed combustion. However, these flames are known to be prone to combustion instabilities, which became the key issue of modern gas turbine combustion research. In this paper, investigations of a single model gas turbine burner are presented with special focus on thermo-acoustic eigenmodes of the combustor and the resulting interaction between periodic flow field oscillations and flame front fluctuations.
A numerical analysis of the eigenmodes of the combustor rig was preformed and compared to pressure probe measurements. By the numerical analysis Helmholtz mode pressure oscillations were predicted to be present in the air plenum upstream the burner as well as in the combustion chamber. These oscillation modes could well be confirmed by the analysis of the pressure signals taken at different position within the combustor rig.
By these pressure oscillations thermo-acoustic flame instabilities are triggered. Due to a phase lag between the pressure oscillations in the air plenum and those in the combustion chamber, fluctuations of air flow through the burner are induced, which in turn cause fluctuations of the equivalence ratio at the burner exit plane. As result, fluctuations of the heat release rate within the flame are established, which interfere with the acoustics of the rig and, thus, unstable combustion is maintained. The dynamics of the flow field and of the flame was studied experimentally by phase-locked LDA and OH-LIF diagnostics. The experimental results give an excellent insight into the chain of processes that are responsible for the thermo-acoustic instabilities. Interestingly, two different oscillation modes could be identified depending on the amplitude of the oscillations. At low oscillation levels only weak and locally confined velocity fluctuations in the main reaction zone were observed which do not have any significant impact on the flame. By increasing the equivalence ratio, the transition from low to high oscillation levels can be triggered. Under high oscillation levels, a pumping motion of the flow field in axial direction could be identified which causes strong periodic disturbances of the flame.

Keywords: thermo-acoustic eigenmode, combustion oscillations, flame instabilities, gas turbine, premixed flames

1. Introduction

Strong limitations of NO_x emissions forced the gas turbine industry to adopt premixed lean combustors which lead to a significant decrease of emissions [3]. However, one drawback of this combustion mode is the high probability of thermo-acoustic instabilities. In recent years, different mechanisms have been identified that cause these instabilities, such as feedback loops between pressure and heat release fluctuations [5], flow instabilities and unsteady air-fuel mixing [12]. All these instabilities can have a major impact on combustion leading to flame front disturbances and fluctuations of the heat release [2, 8] and may significantly compromise the NO_x emissions [7].

The objective of the present study was to identify the mechanisms that are responsible for the thermo-acoustic instabilities of modern heavy duty gas turbines. A transparent test rig with a single model burner of a heavy-duty gas turbine burner was set up. The rig enables detailed experimental investigations at atmospheric pressure.

For non-reacting conditions, a Precessing Vortex Core (PVC) was predicted by LES calculations which is a typical instability of swirling flows [16]. The presence as well the frequency (262 Hz) of the PVC could be confirmed experimentally by HWA measurements in the non-reacting flow in a previous study [13].

Further experimental investigations under reacting conditions revealed the presence of thermo-acoustic instabilities which are by coincidence at almost the same frequency. However, a PVC could not be observed in the reacting flow. In order to clarify the mechanisms of the combustion oscillations, a numerical acoustic eigenmode analysis was performed and the interaction between flame and flow field was investigated experimentally by phase resolved measurements of the flow field by LDA and the flame front by LIF.

2. Nomenclature

A	burner area
c	speed of sound
D	burner outlet diameter
f_H	Helmholtz resonator frequency
HWA	Hot Wire Anemometer
$L,\ l$	length
LDA	Laser Doppler Anemometer
LES	Large Eddy Simulation
LIF	Laser-Induced Fluorescence
l, m, n	mode order in each direction
p	pressure perturbation
$\bar{p},\ p_0$	mean pressure
$\tilde{p}$	period. fluctuation pressure component
$\hat{p}$	pressure amplitude
PVC	Precessing Vortex Core
max	maximum value
r	radius
T	temperature
u	(axial) velocity
$\bar{u}$	mean axial velocity component
$\tilde{u}$	periodical axial velocity component
V	volume
w	circumferential velocity
x, y, z	Karthesian co-ordinate axis
γ	local ratio of heat capacities
φ	phase angle
Φ	equivalence ratio
$\dot{\omega}_T$	local unsteady heat release

3. Burner, Test Rig and Operating Conditions

3.1. Burner

For the present study a single burner (Fig. 1) which mimics a typical design of a heavy duty gas turbine burner was used. It was fired by natural gas. The burner can be operated with either non-premixed or premixed mode gas injection. In addition, the burner is equipped with a pilot gas nozzle which is used to stabilize the premixed flame. The air passage consists of two concentric annular air swirlers. The inner one is equipped with nozzles for pilot gas and non-premixed gas injection. In case of non-premixed operation, the natural gas is injected through the non-premixing nozzles. In premixed mode operation, the premixing gas nozzles and optionally to a minor part the pilot nozzles are used. In both modes, the air is fed through the axial as well as the diagonal swirling ducts with the same flow split. The Reynolds number at the burner outlet is 10^5 and the thermal power can be adjusted from 420 kW at $\Phi = 0.5$ to 770 kW at $\Phi = 0.83$.

3.2. Test Rig

The burner was implemented into a single burner test rig operating at atmospheric pressure. The combustor housing provided access for optical diagnostics such as LIF imaging and LDA. Fig. 2 shows a sketch of the combustor. The combustion chamber has a square cross-section with a truncated pyramidal shape at the outlet. If the diameter of the burner outlet is D (Fig. 1), the overall length of the combustor is $5.5D$ and the width of the square cross-section is $2.9D$. All results of the experimental investigations reported in this paper are based on the co-ordinate system given in Fig. 2 where the burner axis corresponds to the x-axis. In addition, the LIF and LDA measurement planes are shown. The calculations of the acoustic eigenmodes were based on the same geometry.

3.3. Operating Conditions

In premixed mode two different operating points where combustion oscillations are present were investigated: First, a strongly oscillating flow at $\Phi = 0.83$

and, second, a weakly oscillating flow at $\Phi = 0.71$. In both cases, the air volume flow was identical and set to that of a burner in the engine under typical pressurized operating conditions in order to ensure Mach number similarity. In addition, the combustion air was preheated to 673 K which corresponds to a typical burner inlet temperature. In the gas turbine, the burner is operated in premixed mode with pilot gas injection for better flame stability. In order to prevent any disturbance of the premixed flame by the pilot burner under test rig conditions, no pilot gas flow was used during all investigations.

4. Numerical analysis of the acoustic eigenmodes

A useful step for understanding the flame/combustion interaction with acoustic pressure oscillations is to compute the eigenmodes of the full combustor. By linearizing the reactive Navier-Stokes equations around a mean state (index 0), the general Helmholtz equation for acoustic perturbations in a turbulent and reacting flow [4, 10] is obtained:

$$\nabla \cdot \left(c^2 \nabla p\right) - \frac{\partial^2 p}{\partial t^2} = -(\gamma - 1)\frac{\partial \dot{\omega}_T}{\partial t} - \gamma p_0 \nabla \vec{u} : \nabla \vec{u} \tag{1}$$

where p is the pressure perturbation, $\dot{\omega}_T$ is the local unsteady heat release, p_0 is the average pressure and γ and c are the local ratio of heat capacities and speed of sound, respectively. Eq. 1 is derived under the following assumptions:

- low Mach number flow,
- no volume forces,
- small perturbations (i.e. linear acoustics)
- and homogeneous mean pressure.

A detailed presentation of the solver used for Eq. 1 in the frequency domain (assuming harmonic pressure-fluctuations) can be found in [1]. This tool is referred to as the Helmholtz solver.

In reacting flows both γ and c may undergo drastic spatial variations due to changes in composition and temperature. Three-dimensional (3D) fields of c and γ are the input for the Helmholtz solver, which then provides the 3D shape of the mode as well as its frequency and amplification/attenuation rate. For the present study, the 3D fields of c and γ correspond to the averaged fields of a validated Large-Eddy Simulation [15, 16] that duplicates the experiment running in premixed mode at an equivalence ratio $\Phi = 0.5$. The domain for which the eigenmodes are sought consists in the combustion chamber together with the burner and the intake plenum. By the acoustic boundary conditions zero pressure fluctuations are imposed at the chamber outlet ($p = 0$) and zero velocity fluctuations ($u = 0$) at the inlet of the air-box plenum and on all walls. When combustion instabilities occur, turbulence generated noise ($\nabla \vec{u} : \nabla \vec{u} = 0$) can be neglected. The active effects of the flame were also neglected in this work ($\frac{\partial \dot{\omega}_T}{\partial t} = 0$) so that the stability of a given mode can not be predicted. The Helmholtz solver provides all possible acoustic modes but does not indicate which one will actually be excited.

The frequencies of the eigenmodes predicted by the Helmholtz solver are listed in Tab. 1. As standard notations for single-duct acoustic-modes (that is (l, m, n) where l, m and n are the order of the mode in each direction) can hardly be used for multiple ducts, the modes are simply numbered according to their frequency magnitude. The detailed discussion on the structure of all modes is postponed to a further study as the focus is set on the mode which matches the experimentally unstable frequency: mode number 2. The modulus and phase of p are presented in Fig. 3. This mode is characterized by high pressure fluctuation levels in the plenum and somewhat lower levels in the combustion chamber, as well as a phase shift of π at the burner exit. These characteristics are to be compared with measurements on the experimental setup. Also these characteristics show that mode number 2 corresponds to an oscillating mode between the plenum and the chamber with higher pressure fluctuations in the plenum: it can be compared to a Helmholtz resonator with the plenum being the container and the burner being the neck.

The Helmholtz frequency f_H of the plenum and the attached burner [1] is given as

$$f_H = \frac{c}{2\pi}\sqrt{\frac{A}{L \cdot V}} \tag{2}$$

where A is the area of the burner, L its corrected length of the burner and V the volume of the plenum. The corrected length [10] is set to $L = l + r$, l being the actual neck length and r its radius. For this configuration, Eq. 2 gives a frequency of $f_H = 247.9$ Hz. Consequently, the conjecture of the unstable frequency as being the Helmholtz resonator frequency of the plenum is supported by three facts:

- it is close to f_H,
- it varies as the square root of the plenum temperature consistently with Eq. 2
- and it does not depend on Φ and the temperature in the combustion chamber [14].

5. Verification of Acoustic Eigenmode by Pressure Measurements

For the both combustion oscillation modes to be discussed in the next section, the dominant frequency was found to be at 251-255 Hz which is almost identical to the predicted eigenmode number 2 at 249.7 Hz. The corresponding Helmholtz resonator mode was verified experimentally by pressure probe measurements. The signals of two pressure transducers were recorded simultaneously. One was equipped with an infinite coil probe [9] and consecutively mounted at different axial and angular positions of the combustor wall (Fig. 4). The other transducer was located in the

air plenum and its signal was used as reference signal for phase angle matching.

The pressure fluctuations recorded at different axial and angular positions are plotted versus the phase angle in Fig. 5 for the strong oscillation mode and and in Fig. 9 for the weak oscillation mode. From the pressure signals two conclusions can be drawn: First, the pressure signals from all circumferential positions at constant axial position are in phase, which is a clear indication that no PVC is present under reacting conditions. This was also confirmed by phase-locked LDA measurements at different angular positions. Second, no phase lag was found between the pressure signals at different axial position which confirms the predicted Helmholtz mode within the combustor. The observation of nearly identical pressure amplitudes at different axial positions excludes the presence of a quarter-wave mode.

Additionally, also the fluctuation of the pressure difference between the plenum and the burner which actually is the fluctuating pressure difference across the burner is shown in Figs. 5 and 9. As both, the pressure inside the air plenum as well as the pressure inside the combustor are normalized to the corresponding mean value, the pressure fluctuation across the burner becomes negative for some phase angle regimes. In contrast the eigenmode calculations, where a phase lag of $\Delta\varphi = 180^\circ$ (Fig. 3) across the burner was predicted, the experiment gives a phase lag of 77.5° for the strong oscillation mode and $\Delta\varphi = 57^\circ$ for the weak oscillation mode. The discrepancy between experiment and prediction may be attributed to the fact that the damping within the neck, i.e. friction losses within the burner were neglected, and also the presence of the flame was not accounted for in the calculations. The wiggles with a frequency of about 10 kHz in the pressure records taken inside the combustor (Fig. 5) are caused by signal processing. However, Fourier transforms of all pressure signals did not reveal a pronounced peak at this frequency.

In order to verify that the Helmholtz resonator where the air plenum acts as resonator and the burner as neck is relevant oscillator, additional experimental investigations where performed: The resonance frequency of this Helmholtz resonator is linearly proportional to the speed of sound inside the air plenum and, therefore, to $\sqrt{T_{Plenum}}$. A variation of temperature of the air supplied to the air plenum between 573 K and 673 K revealed oscillation frequencies from 231 Hz to 252 Hz [13] which complies exactly to what is predicted by Eq. 2. On the other hand, a variation of the temperature and, thus the speed of sound inside the combustion chamber by changing the fuel flow at constant air flow and constant air inlet temperature did have no effect on the frequency of the oscillations. This is prove that the combustion chamber does not act as resonator for the present eigenmode. Thus, there is clear evidence that the predicted Helmholtz resonator mode triggers the observed combustion oscillations.

6. Flow Field - Flame Interaction

When operating the test rig under conditions typical for gas turbines, the flame does not pulsate. However, by increasing the equivalence ratio beyond the typical operation range, the stability limit is exceeded and the flame starts to oscillate. Because of the higher wall temperatures in the test rig which is not equipped with film cooled walls, and also because of the missing interaction with the adjacent burners, the combustion rig acts sightly different in terms of stability limits compared to the gas turbine.

When the equivalence ratio is increased beyond the stability limit, the amplitudes of the dynamic pressure fluctuations start to grow steadily. First audible instabilities are established at $\Phi \geq 0.71$ ($\tilde{p}/\bar{p} \approx 0.0008$). Inbetween $\Phi = 0.75$ and $\Phi = 0.80$ a transient regime was found where the pressure amplitudes jump between high and low over time, even for constant operation condition settings. Beyond an equivalence ratio of $\Phi = 0.80$ only high amplitude pressure oscillations are present. It should be noted that both types of oscillations have the same frequency.

Both instability modes are governed by a common basic mechanism: Due to the phase lag between the pressure fluctuations in the air plenum and combustor, an alternating acceleration and deceleration of the air flow through the burner in induced. The fuel is injected into this air flow with high subsonic speed. The fuel injection nozzle is nearly choked and, therefore, the fuel flow is approximately constant. As consequence, fuel rich and fuel lean pockets are generated in the premixing passage of the burner. When these pockets are convected downstream into the combustor and finally reach the flame, fluctuations of the heat release and flow pulsations are induced which in turn trigger the combustion oscillations. However, the resulting flow instabilities and their interaction with the flame are significantly different for the two instability modes. The flow - flame interaction of both modes will be discussed in detail subsequently.

6.1. High Oscillation Amplitudes

For analyzing the mechanism at high oscillation amplitudes, an operation point at $\Phi = 0.83$ was selected, where pressure fluctuations at 254 Hz with an amplitude of $\tilde{p}/\bar{p} = 0.015$ are found in the combustor [14].

The reacting flow was investigated by LDA and OH LIF. Similarly to the previously described pressure fluctuation measurements, the signal of the pressure sensor in the air plenum (Fig. 4) was used as reference for synchronizing the LDA burst spectrum analyzers [14] and the LIF system. Thus, all phase angles are referenced to the pressure signal in the plenum (Fig. 5).

The phase-locked axial velocity is plotted in Fig. 6 for four different phase angles, normalized by the maximum of the mean axial velocity $\bar{u}_{max}$. At

$\varphi = 276^\circ$ regions of high positive axial velocities ($u/\bar{u} = 1.14$) are generated in the main flow ($x/D = 0.4,\ y/D = 0.6$). Then these accelerated flow pattern move downstream ($\varphi = 6^\circ, 96^\circ$) and finally are dissipated ($\varphi = 186^\circ$). Velocity fluctuations can also be found in the recirculation zone which are in phase to those of the main flow. Therefore, the unsteady flow field can be described as a pumping motion in axial direction.

Fig. 7 shows OH LIF intensities which are phase averaged over 400 single exposures. The flame front may be assumed to be located close to the steepest OH gradient [6]. The LIF images are superimposed by phase-averaged axial velocities ($\bar{u} + \tilde{u}$) plots. The LIF data show that the flame is located inbetween the recirculation zone and the main flow close to the zero velocity iso-line which is indicated by the dashed line in the plots. In this region high velocity gradients and strong velocity fluctuations prevail and, thus, the flame is very sensitive to changes of the flow field. It is obvious from the plots that the flame strongly fluctuates during one period of oscillation. At phase angles of $\varphi = 2^\circ$ and 92° the flame is nearly undisturbed. At phase angles of $\varphi = 182^\circ$ and 272° we have a strongly disturbed flame, where no OH gradients are present indicating the absence of a well-defined flame front.

In order to elucidate the interaction of the pressure fluctuations and the oscillations of the velocity field with the flame, we first focus on the phase angle regime $\varphi = 182^\circ - 272^\circ$ where the flame is strongly perturbed. Obviously, the disturbed flame causes are significant reduction of the heat release, and as consequence the local density increases and the axial velocity within the flame zone decreases. Due to the reduced axial momentum flux, the swirl number within the flame region ($x/D = 0.633$) starts to increase as shown in Fig. 8 [11, 14]. Therefore, deteriorated mixing within the shear layer because of reduced axial velocity gradients and a significant reduction in axial velocity which in tendency causes the flame to propagate upstream, may be the reasons why there is no well-defined flame front.

On the other hand, the pressure difference across the burner is less than the temporal mean value starting from $\varphi \approx 210^\circ$. Thus, a fuel richer mixture is generated in the burner premixing passage. When these fuel rich pockets reach the flame zone at $\varphi \approx 300^\circ$, the flame recovers. As consequence, the heat release increases and the pressure in the combustor rises (Fig. 5). Due to the enhanced heat release, the local density decreases and the axial velocity within the flame zone rises, which cause the flame to be deflected slightly downstream. Thus, in the strong oscillation mode, we have a strong disturbance of the flame associated with slight deflection of the flame in axial direction.

6.2. Low Oscillation Amplitudes

As described previously, weak oscillations with approximately 20 times lower pressure oscillation amplitudes were present between $\Phi = 0.71$ and $\Phi = 0.75$. The flow field - flame interaction of those oscillations were investigated at $\Phi = 0.71$ with an air flow and air inlet temperature identical to that of the strongly oscillating flow. Similarly as for strong oscillations, a phase shift between the pressure fluctuations in the plenum and the combustor was observed but with a smaller phase lag of $\Delta\varphi = 57^\circ$ (Fig. 9). The minimum pressure difference and, hence, the lowest velocity through the burner was found at $\varphi = 310^\circ$. At this phase angle fuel rich bubbles are generated inside the burner diagonal swirler blades [13], which are convected downstream and emerge from the burner outlet (Fig. 1) at $\varphi = 439^\circ$ ($\varphi = 79^\circ$).

The normalized mean axial velocity together with the superimposed time lag distribution (shown as isolines) is plotted in Fig. 10. The velocities were captured by LDA, and from the velocity field the local time lag was calculated which is referenced to a zero value at the burner outlet. The time lag field reveals that fuel inhomogeneities emerging from the burner mouth will arrive approximately 2 ms later at the main reaction zone. This delay corresponds to $\Delta\varphi \approx 180^\circ$ for oscillations at 251 Hz. Thus, at $\varphi = 79^\circ + 180^\circ = 259^\circ$ the heat release in the flame reaches its maximum.

The velocity fluctuation have been extracted from the LDA measurements and plotted in Fig. 11 for two phase angles: $\varphi = 268^\circ$ which represents approximately the phase angle at maximum heat release within the flame zone, whereas $\varphi = 88^\circ$ corresponds to approximately minimum heat release. The contours represent the amplitude of the periodical axial velocity fluctuation $\tilde{u}/\bar{u}_{max}$, the iso-lines the mean value of the axial velocity $\bar{u}/\bar{u}_{max}$. It is evident from the plots that the fluctuations are locally confined to the main reaction zone at $x/D = 0.6$, $y/D = 0.5$. For $\varphi = 268^\circ$ strong velocity fluctuations are present in the reaction zone , whereas for $\varphi = 88^\circ$ only minimal velocity fluctuations are found. Thus, the velocity fluctuations inside the flame zone are almost in phase with heat release.

As the fluctuations of the velocity are comparably small there is just a minor impact on the flame, which is confirmed by the OH-LIF intensity plots in Fig. 12. The flame is still sufficiently stabilized by the swirl [14] and the flame position as well as the shape does not vary.

7. Conclusion

The mechanisms leading the thermo-acoustic oscillation of the single premixed, swirl stabilized gas turbine model combustor were studied by extensive experimental investigations. By an accompanying numerical study of the acoustic eigenmodes of the test rig, an Helmholtz mode where the air plenum acts as resonator and the burner air passage as neck could be identified as relevant eigenmode.

This Helmholtz mode could be confirmed in the experiment by investigating the pressure oscillations at different position inside the combustion chamber, as well as by analyzing the velocity fluctuations by LDA and the flame perturbation by LIF inside. Furthermore, by varying the temperature either inside the air plenum or inside the combustion chamber, the air plenum could be proven to be the resonator of the system.

Depending on the setting of the equivalence ratio at otherwise identical operation conditions, two different modes of oscillation at the same frequency could be discriminated in the experiments. The two oscillation modes differ mainly in the amplitude of the associated pressure fluctuations. For both oscillation modes, the Helmholtz resonator mode could be identified as the driving acoustic feedback mechanism. As consequence of the phase shift of the pressure fluctuations across the burner, velocity fluctuations through the air passage of the burner are induced, by which in turn fluctuations of the equivalence ratio of the flow emerging from the burner are generated. When the alternating patterns of fuel rich and lean pockets reach the flame zone, the heat release starts to fluctuate, and fluctuations of density as well as the axial velocity within the flame zone are established.

In the case of low oscillation amplitudes, the phase lag across the burner was $\Delta\varphi = 57^\circ$. Minor fluctuations of the axial velocity inside the flame zone could be identified in the experiment. But the LIF data revealed that the flame itself was nearly undisturbed by the velocity field fluctuations.

In the case of strong oscillations, the phase lag across the burner was higher ($\Delta\varphi = 77.5^\circ$). Strong fluctuations of the axial velocity inside the flame zone were found which cause a periodic disturbance of the flame and a local break down of the nominal swirl number within the flame zone [13]. As consequence, the flame nearly seems to extinguish over a phase angle range of almost $\Delta\varphi \approx 90^\circ$.

Acknowledgments

This study was partially supported by the EC under contract ENK5-CT-2000-00060 (PRECCINSTA) which is gratefully acknowledged.

References

[1] L. Benoit, F. Nicoud, *Numerical Assessment of Thermo-Acoustic Instabilities in Gas Turbines, Int. J. Num. Meth. In Fluids* 47 (2005) 849-855.

[2] C. M. Coats, *Coherent Structures in Combustion, Prog. Energy Combust. Sci.* 22 (1997) 427–509.

[3] S. M. Correa, *A Review of NO_x Formation under Gas-Turbine Combustion Conditions, Combustion Science and Technology* 87 (1-6) (1992) 329–362.

[4] D. G. Crighton, A. Dowling, J. Ffowcs Williams, M. Heckl, F. Leppington, *Modern Methods in Analytical Acoustics*, Springer Verlag, New-York, 1992.

[5] W. Krebs, P. Flohr, B. Prade, S. Hoffmann, *Thermoacoustic Stability Chart for High Intense Gas Turbine Combustions Systems, Combustion Science and Technology* 174 (7) (2002) 99–128.

[6] T. Langenfeld, A. Kremer, E. P. Hassel, J. Janicka, T. Schäfer, J. Kazenwadel, C. Schulz, J. Wolfrum, *Laserdiagnostic and Numerical Studies of Strongly Swirling Natural-Gas Flames, Proc. Comb. Inst.* 27 (1998) 1023–1030.

[7] J. A. Miller, C. T. Bowman, *Mechanism and Modeling of Nitrogen Chemistry in Combustion, Prog. Energy Combust.* 15 (1989) 287–338

[8] C. J. Mueller, J. F. Driscoll, D. L. Reuss, M. C. Drake, M. E. Rosalik, *Vorticity Generation and Attenuation as Vortices Convect Through a Premixed Flame, Combustion and Flame* 112 (1998) 342-358.

[9] J. Mahan, A. Karchmer, *Combustion Core Noise, Aeroacoustics of Flight Vehicles: Theorie and Practice* NASA Langley Research (1991).

[10] T. Poinsot, D. Veynante, *Theoretical and Numerical Combustion*, 2nd Edition, R.T. Edwards, 2001.

[11] W. Polifke, A. Fischer, T. Sattelmayer, *Instability of a Premix Burner with Non-Monotonic Pressure Drop Characteristic, ASME-Paper 2001-GT-0035* (2001).

[12] G. Richards, D. Straub, *Control of Combustion Dynamics using Fuel System Impedance, ASME-Paper GT2003-38521* (2003).

[13] K.-U. Schildmacher, R. Koch, H.-J. Bauer, *Experimental Characterization of Premixed Flame Instabilities of a Model Gas Turbine Burner, accepted for publication in the Journal of Flow, Turbulence and Combustion* (2006).

[14] K.-U. Schildmacher, R. Koch, *Experimental Investigations of the Interaction of Unsteady Flow with Combustion, Journal of Engineering for Gas Turbines and Power* 127 (2) (2005) 295–300.

[15] L. Selle, L. Benoit, T. Poinsot, W. Krebs, *Joint use of Compressible Large-Eddy Simulation and Helmholtz solvers for the analysis of rotating modes in an industrial swirled burner, Combustion and Flame, in press*

[16] L. Selle, G. Lartigue, T. Poinsot, R. Koch, K.-U. Schildmacher, W. Krebs, P. Kaufmann, D. Veynente, *Compressible Large Eddy Simulation of Turbulent Combustion in Complex Geometry on Unstructured Meshes, Combustion and Flame* 137 (4) (2004) 489–505.

Table 1: List of eigen-frequencies as computed by the Helmholtz solver

Frequency [Hz]	Mode number
134.7	1
249.7	2
763.2	3
936.1	4
936.1	5
982.3	6
1186.8	7
1186.9	8

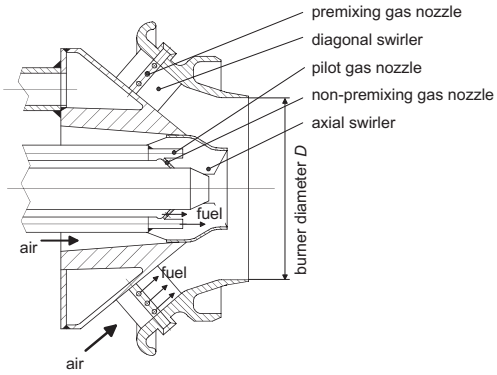

Figure 1: Sketch of the burner

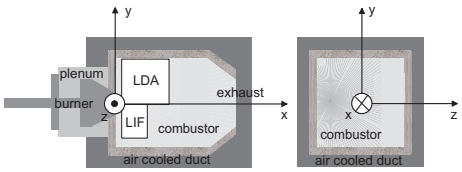

Figure 2: Sketch of the combustor and co-ordinate system

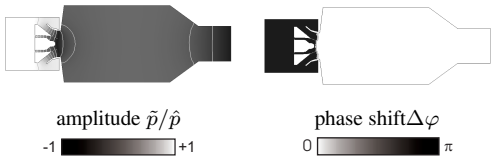

Figure 3: Calculated pressure fluctuations in the plenum and combustor

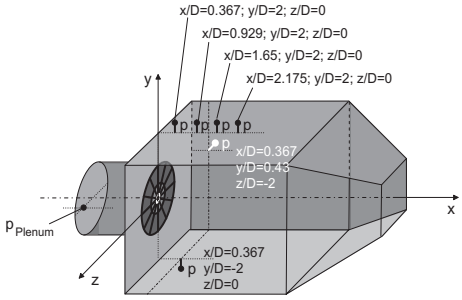

Figure 4: Positions of pressure measurements

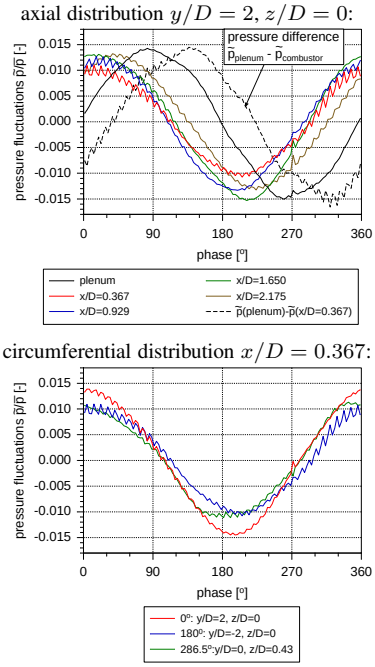

Figure 5: Phase-locked pressure distribution in the plenum and combustor ($\Phi = 0.83$)

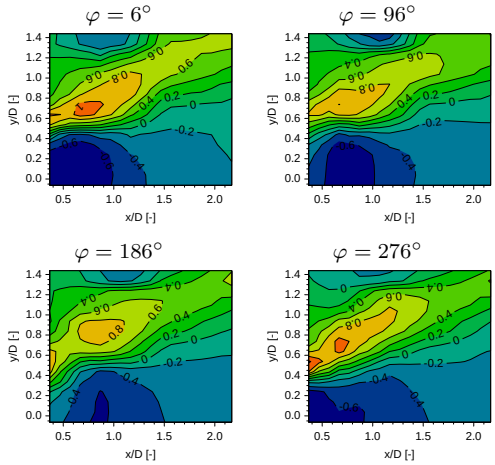

Figure 6: Phase-locked axial velocity field ($\Phi = 0.83$)

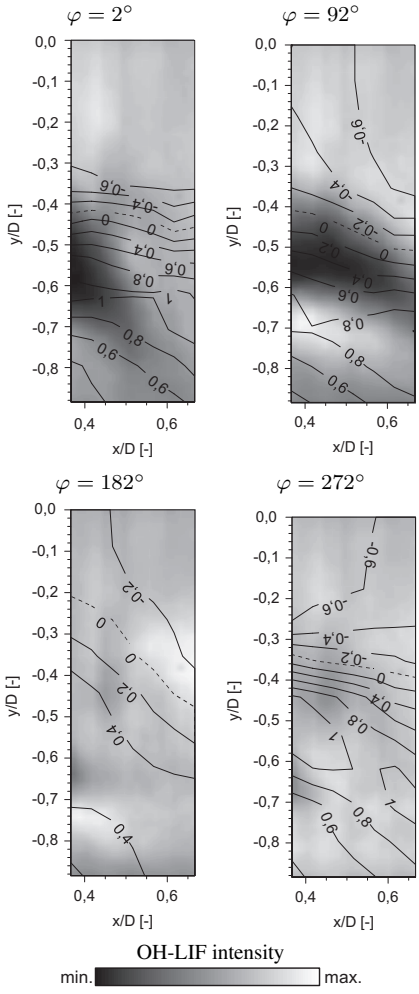

Figure 7: Phase-locked OH-LIF intensities with superimposed axial velocity isolines ($\Phi = 0.83$)

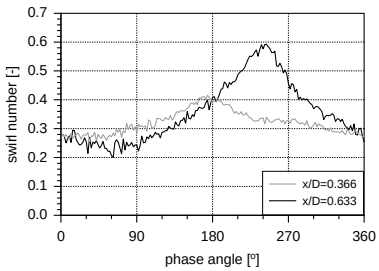

Figure 8: Fluctuations of the swirl number ($\Phi = 0.83$)

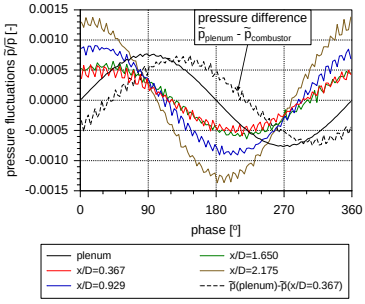

Figure 9: Phase-locked pressure distribution in the plenum and combustor ($\Phi = 0.71$)

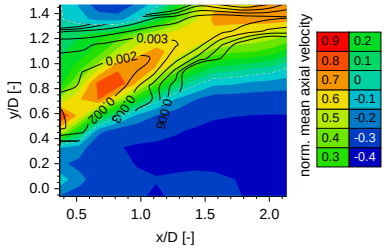

Figure 10: Mean axial velocity with superimposed time lag isolines in sec. ($\Phi = 0.71$)

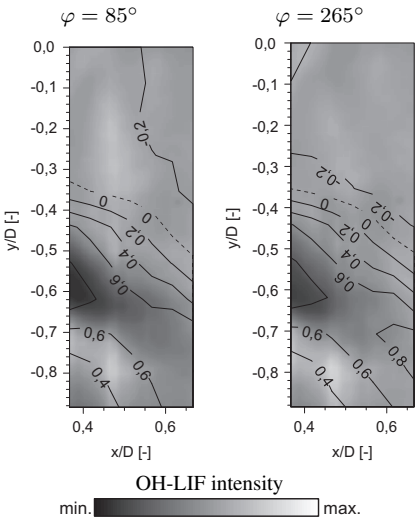

Figure 12: Phase-locked OH-LIF intensities with superimposed axial velocity isolines ($\Phi = 0.71$)

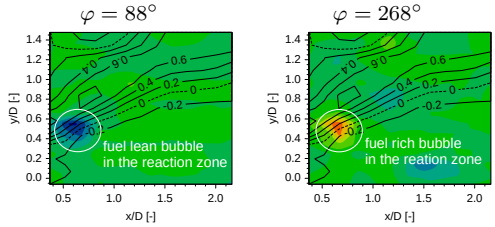

Figure 11: Periodical axial velocity fluctuations and superimposed mean axial velocity field ($\Phi = 0.71$)